RNA (1996), 2:611-621. Cambridge University Press. Printed in the USA.

Detection of double-stranded RNA–protein interactions by methylene blue-mediated photo-crosslinking

ZHI-REN LIU,[1] ARLENE M. WILKIE,[2] MICHAEL J. CLEMENS,[2] and CHRISTOPHER W.J. SMITH[1]

[1] Department of Biochemistry, University of Cambridge, Tennis Court Road, Cambridge, CB2 1QW, United Kingdom
[2] Division of Biochemistry, Department of Cellular and Molecular Sciences, St George's Hospital Medical School, Cranmer Terrace, London, SW17 0RE, United Kingdom

ABSTRACT

Double-stranded (ds) RNA-binding proteins have diverse functions in the cell. An obstacle to investigating the interactions between these proteins and dsRNA is the relative inefficiency of traditional UV-crosslinking methods for extended regions of dsRNA. We have therefore developed an alternative procedure for RNA–protein photo-crosslinking that efficiently induces RNA–protein crosslinks in double-stranded regions of RNA. We show that dsRNA–protein crosslinks can be induced by visible light in the presence of the dye methylene blue, which most likely mediates crosslinking by intercalating in the dsRNA helix. A recombinant dsRNA binding domain from the *Drosophila* staufen protein and human protein kinase R were crosslinked by UV or methylene blue to a series of dsRNAs. In each case, the degree of crosslinking was greater with methylene blue, particularly with RNAs with few single-stranded loops. Methylene blue-mediated crosslinking therefore complements and extends the existing repertoire of crosslinking methods for detecting RNA–protein interactions.

Keywords: crosslinking; double-stranded RNA; methylene blue

INTRODUCTION

Double-stranded (ds) RNA-binding proteins play important roles in various cellular processes, including regulation of transcription and translation, RNA editing, mRNA degradation, mRNA localization, and cellular antiviral activities. (Cattaneo, 1994; Bass, 1995; Proud, 1995). Many of these proteins bind to dsRNA with little or no primary sequence specificity (Bass et al., 1994). This property of dsRNA-binding proteins reflects the structure of the A-form dsRNA helix, which has a deep and narrow major groove in which the bases are not accessible for molecular recognition except at the ends of the helix (Weeks & Crothers, 1993). The exposed functional groups of the bases in the minor groove are relatively information poor and do not allow for discrimination between different base pairs.

A well-characterized example of a dsRNA-binding protein is protein kinase R (PKR) (Proud, 1995; Clemens, 1996). This kinase is activated by auto-phosphorylation upon binding to dsRNA. Its expression is induced by interferon, and it inhibits translation in virally infected cells by phosphorylation of the α-subunit of initiation factor eIF2. Its activity is also regulated by various other molecules, including many viral small RNAs, such as adenovirus VAI RNA, which bind to PKR without subsequent activation of the kinase (Clemens et al., 1994; Jagus & Gray, 1994; Proud, 1995). The staufen protein in *Drosophila* is a more specialized dsRNA-binding protein required for localization of *oskar* and *bicoid* mRNAs to opposite poles of the *Drosophila* egg (St. Johnston et al., 1991; Stebbings et al., 1995; St. Johnston, 1995). Staufen has been shown to associate with a highly structured 400-nt segment of the 3′ untranslated region (UTR) of *bcd* mRNA, and this specific binding is thought to mediate appropriate localization of the mRNA (Ferrandon et al., 1994).

Both PKR and staufen contain copies of a 65-amino acid dsRNA-binding motif that has been identified in many dsRNA-binding proteins (St. Johnston et al., 1992). These motifs constitute modular dsRNA-binding domains (dsRBD) that are able to interact independently with dsRNA (St. Johnston et al., 1992). Recently, the NMR solution structures of individual dsRBDs from staufen and *Escherichia coli* RNase III have been solved (Bycroft et al., 1995; Kharrat et al., 1995). PKR contains two dsRBD domains distinct from the protein kinase domains (Clarke & Mathews, 1995; Green et al., 1995). Mutagenesis studies indicate that the first RBD is more

Reprint requests to: Chris Smith, Department of Biochemistry, University of Cambridge, Tennis Court Road, Cambridge, CB2 1QW, United Kingdom; e-mail: cwjs1@mole.bio.cam.ac.uk.

important for RNA binding (Green et al., 1995). Staufen contains five copies of the dsRNA-binding motif. The multi-copy dsRBD arrangement may be important for conferring specific recognition of RNA structures in the appropriate 3′-UTRs, despite the apparent sequence-independent binding of individual *staufen* dsRBDs to dsRNA (St. Johnston et al., 1992; Bycroft et al., 1995).

Photo-crosslinking is a commonly used method to study RNA–protein interactions. Radiolabeled RNAs are incubated with proteins and then irradiated with suitable wavelength light to induce crosslinking. After treatment with ribonucleases, RNA-binding proteins are identified by SDS-PAGE and autoradiography. Only proteins bound originally to the labeled RNA become radiolabeled subsequently. The conventional method is UV (254 nm)-induced crosslinking (Hanna, 1989). Improvements upon the efficiency and specificity of crosslinking have been made by using photoreactive nucleoside analogues such as 4-thiouridine (Tanner et al., 1988), 5-bromouridine (Gott et al., 1991), 5-iodouridine (Willis et al., 1993), 5-iodo-cytidine (Meisenheimer et al., 1996), and various nucleoside azido derivatives (Wower et al., 1994). In general, photoreactive analogues circumvent irradiation of samples with short-wavelength UV light, significantly reducing nonspecific crosslinking. Site-specific crosslinking can be achieved by means of RNA recombinant techniques, in which photoactive analogues are incorporated into specific sites of an RNA molecule by oligonucleotide-mediated ligation (Moore & Sharp, 1992; MacMillan et al., 1994). These crosslinking techniques have found wide applicability for the study of protein interactions with single-stranded RNA (ssRNA). Although not all of the modified nucleosides have yet been tested with dsRNA, traditional UV-induced crosslinking is often very inefficient for detecting dsRNA-binding proteins. We have therefore set out to develop a simple and efficient procedure for photochemical crosslinking of proteins to dsRNA.

Methylene blue (MB) is a cationic phenothiazinium dye (see Fig. 1A), that has been used widely as a tissue stain dye. MB treatment has long been known to inactivate both viruses and bacteria by photosensitization, the principal cellular target being DNA (reviewed

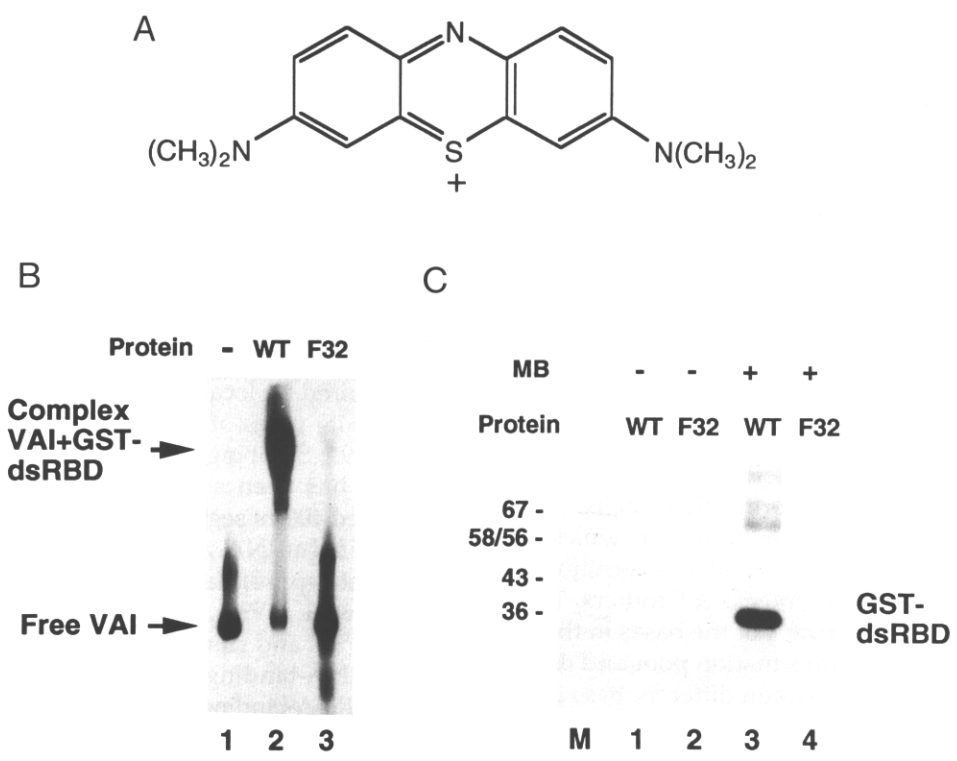

FIGURE 1. A: Structure of methylene blue. Note that the dye is cationic, explaining its ability to bind to nucleic acids both electrostatically with the phosphate backbones as well as by intercalation between the bases. **B:** Electrophoretic gel-mobility shift assay of binding of wild-type GST-dsRBD (WT) and its mutant F32A (F32) to VAI RNA. Labeled VAI RNA (6 ng) was incubated with 150 ng of protein at room temperature. Complex formation was analyzed by 8% native PAGE. Lane 1, free VAI RNA; lane 2, VAI + GST-dsRBD; lane 3, VAI + F32A. Positions of free VAI RNA and RNA–protein complex are indicated beside the autoradiograph. **C:** Assay for MB-mediated crosslinking of GST-dsRBD (WT) and its mutant F32A (F32) to VAI RNA. Labeled RNA and proteins were incubated as in B. Lane 1, GST-dsRBD, no addition of MB; lane 2, F32A, no MB; lane 3, GST-dsRBD + MB; lane 4, F32A + MB; lane M, molecular weight markers. Sizes of markers are indicated to the left. Radiolabeled 37-kDa protein was only detected with GST-dsRBD + MB.

in Tuite & Kelly, 1993). MB photosensitization leads to preferential breakdown of guanine bases. More recently, MB has been shown to mediate visible light-induced DNA–protein crosslinking in chromatin, as indicated by the decrease in A_{260} of samples from which proteins have been removed after MB treatment (Lalwani et al., 1990, 1995). Competition of crosslinking by ethidium bromide indicated that it is dependent upon intercalation of MB between the DNA base pairs (Lalwani et al., 1995). We reasoned that MB might bind to dsRNA and mediate crosslinking to proteins in a similar manner. If so, it should be possible to detect proteins that interact specifically with dsRNA by transfer of radiolabel from RNA to protein after crosslinking and subsequent nuclease digestion. In this report, we demonstrate that MB can be used to detect dsRNA–protein interactions by visible light-induced crosslinking. We show that both a recombinant staufen dsRBD and purified PKR can be MB crosslinked to various dsRNAs. In general, the efficiency of MB crosslinking correlates inversely with that of UV crosslinking. Although UV crosslinking is much more efficient for ssRNA, MB crosslinking is highly dependent upon the presence of base paired dsRNA and is considerably more efficient than UV-induced crosslinking for highly structured dsRNA, with crosslinking efficiencies of 10–15% being readily observed. Thus, MB crosslinking may serve as a complementary method for detecting RNA–protein interactions that are not readily detectable by traditional methods.

RESULTS

Development of MB crosslinking procedure

To initially develop the MB crosslinking procedure, a recombinant GST fusion protein with the third dsRBD from staufen (GST-dsRBD) and a mutant with phenylalanine 32 replaced by alanine (F32A) were tested for binding to adenovirus VAI RNA. Previous studies have shown, by north-western blot and electrophoretic mobility shift, that GST-dsRBD, but not the F32A mutant, binds to the dsRNA 3′-UTR of *bicoid* mRNA and to adenovirus VAI RNA (Bycroft et al., 1995). We verified these binding properties by a gel mobility-shift assay using the two recombinant proteins and labeled VAI RNA. Recombinant protein (150 ng) was incubated with 6 ng of radiolabeled VAI RNA prior to native gel electrophoresis. Only the wild-type protein produced a retarded protein–RNA complex (Fig. 1B). The excess of protein (~0.4 μM) over RNA (~0.01 μM) was presumably required due to relatively weak binding of the individual dsRBD to dsRNA (estimated K_D = 100 nM, data not shown). A typical MB crosslinking experiment is shown in Figure 1C. The same quantities of RNA and protein as in Figure 1B were subsequently incubated with 5 ng of MB and exposed to visible light irradiation. The 37-kDa GST-dsRBD could be detected readily by MB crosslinking under visible light irradiation (Fig. 1C, lane 3), whereas crosslinking of the F32A mutant was undetectable (lane 4). Coomassie blue staining confirmed that both proteins were present at the same level (data not shown). Thus, the MB crosslinking results exactly paralleled the mobility shift data. Crosslinking required irradiation of light on the samples. No crosslinking signal was detected when GST-dsRBD was incubated with VAI in the presence of MB in the dark (data not shown).

In order to investigate the optimum conditions for MB crosslinking, we tested the effects of varying MB dosage, time of light irradiation, and salt concentration. Even with only 0.1 ng of MB (0.01 ng/μL), corresponding to one MB molecule per 60 RNA bases, some crosslinking was detected (Fig. 2A, lane 2). Optimal crosslinking was obtained in the range of 2–10 ng (0.2–1 ng/μL), corresponding to an RNA base:MB ratio of 3–0.6:1

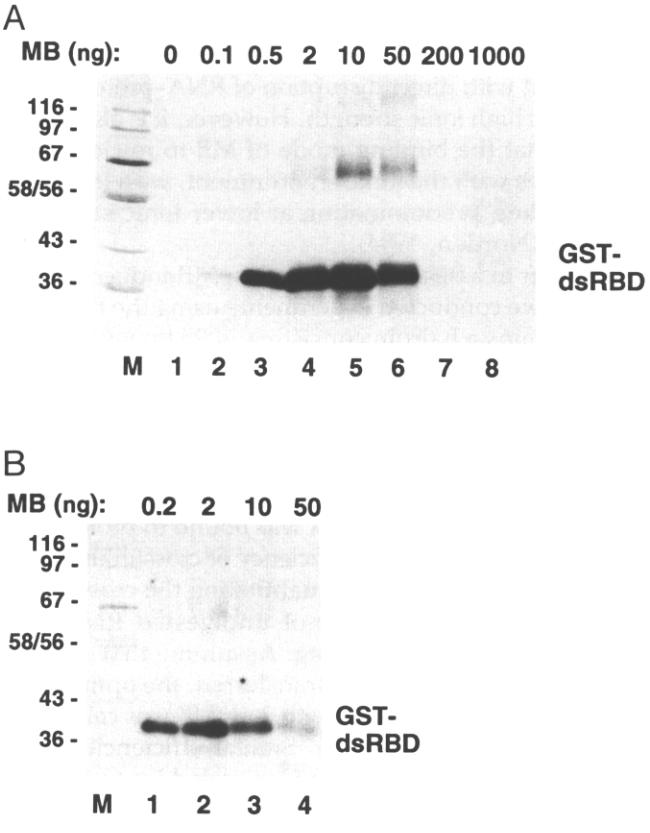

FIGURE 2. Titration of MB in crosslinking reactions. **A:** Crosslinking was conducted with labeled VAI RNA (6 ng) and GST-dsRBD (150 ng) with the indicated amounts of MB (0–1,000 ng, lanes 1–8). Sizes of markers are indicated to the left of the marker lane, M. Optimal crosslinking of monomeric GST-dsRBD occurred with the addition of 2–10 ng MB (lanes 4, 5). **B:** Crosslinking was conducted as in A, but with 6 ng of HP RNA. Crosslinking was quantitated by phosphorimaging of the gel, including a sample of undigested RNA. Crosslinking efficiencies were calculated to be 7.0, 12.0, 8.0, and 3.5% in lanes 1–4, respectively. The optimal crosslinking (12%) was obtained with 2 ng of MB.

(Fig. 2A, lanes 4, 5). Two weaker bands of lower mobility were noticeable, particularly at intermediate MB concentrations (Fig. 2A, lanes 4–6). The mobility of these bands corresponds to ~71 kDa and 120 kDa, suggesting that they arise from crosslinking of GST-dsRBD dimers and trimers. These could possibly have arisen through MB-mediated crosslinking of GST-dsRBD monomers bound to the same dsRNA molecule. High concentrations of MB abolished crosslinking completely (lanes 7, 8). This is likely due to MB interference with protein binding at high concentrations. Gel mobility shift assays confirmed that concentrations of MB below 2.5 ng/μL had no effect, whereas higher MB doses interfered with binding (data not shown).

We found that the crosslinking signal was not increased significantly by prolonging light irradiation after 6 min (data not shown). Neither was crosslinking affected by changes in ionic conditions that would be used commonly in studying RNA–protein interactions. The crosslinking signal was unaffected between 2 and 10 mM Mg^{2+}, and was slightly reduced at 25 mM Mg^{2+}. No effects on crosslinking were detected up to 150 mM NaCl, but crosslinking was completely abolished at 500 mM NaCl (data not shown). These data are consistent with direct disruption of RNA–protein interactions at high ionic strength. However, it is also worth noting that the binding mode of MB to nucleic acids also varies with the ionic environment, with intercalative binding predominating at lower ionic strengths (Tuite & Norden, 1994).

In order to assess the efficiency of MB-induced crosslinking, we conducted experiments using the RNA HP that contains a hairpin consisting of 25 bp with a 4-bp loop, which would be expected to bind a single dsRBD (Fig. 2B). This RNA also produced a clear 37-kDa crosslinked band, with an apparent optimal MB concentration (2 ng/10 μL) slightly lower than for VAI RNA. Because the experiments were performed under conditions in which all the RNA was bound to protein, we were able to estimate the efficiency of crosslinking with respect to bound RNA by quantitating the crosslinked bands alongside a sample of undigested RNA (not shown) by phosphorimaging. Assuming that a single radio-labeled phosphate is transferred, the optimal observed efficiency obtained with 2 ng MB was calculated to be 12% (Fig. 2B, lane 2). Similar efficiencies were obtained when the reaction was scaled up to include 100 ng of protein, 100 ng of RNA, and 50 ng of MB in the same reaction volume, suggesting that it should be feasible to investigate the sites of MB-induced crosslinking in the RNA and protein.

MB does not mediate RNA–RNA or ssRNA–protein crosslinking

The preceding data demonstrated that MB could mediate covalent dsRNA–protein crosslinking. We next investigated whether MB also induces RNA–RNA crosslinks in double-stranded regions. We transcribed complementary RNAs from the polylinker region of plasmid pSP70 (pSP70/*Bgl* II and pSP70/*Xho* I, respectively). The transcript from pSP70/*Bgl* II was radiolabeled and was synthesized using either UTP or the photoreactive analogue 4-thio UTP. After annealing the complementary RNAs, the hybrid was subjected to MB, UV, and trioxsalen crosslinking experiments. MB treatment did not induce RNA–RNA crosslinking, as shown by the mobility of the RNA band in denaturing PAGE (Fig. 3A, lane 2). Only a trace amount of RNA was crosslinked when the MB dosage was increased 50 times (lane 3). On the other hand, RNA–RNA crosslinking was achieved by either UV (305 nm) irradiation of the 4-thiouridine-containing RNA (lane 4) or by trioxsalen crosslinking (lane 5). These data demonstrate that MB does not mediate RNA–RNA crosslinking.

We next investigated whether the MB crosslinking method can efficiently detect interactions of proteins with ssRNA. We used a fusion protein of the *Drosophila* splicing regulator sex-lethal (Sxl) fused to a GST domain (GST-Sxl). Sxl is an ssRNA-binding protein that regulates splicing by binding to uridine-rich sequences (Valcárcel et al., 1993; Wang & Bell, 1994; Singh et al., 1995). A transcript containing an Sxl-binding site was transcribed from a Bluescript SKII vector. Binding of GST-Sxl to this transcript was confirmed by gel-shift assays (data not shown). The protein was crosslinked readily to the target RNA by UV-induced crosslinking (Fig. 3B, lane 2). However, almost no crosslinking was detected upon visible light irradiation in the presence of MB (Fig. 3B, lane 1). This result is consistent with MB crosslinking requiring intercalation of MB into dsRNA. An alternative possibility is that the uridine-rich Sxl binding site does not have a suitable base composition for MB crosslinking. This seems unlikely, because the binding site contains two guanine bases that are thought to mediate the photosensitization of nucleic acids (Tuite & Kelly, 1993; also see the Discussion). Moreover, we have subsequently found that La protein (Chan & Tan, 1987; Gottlieb & Steitz, 1989) can be crosslinked efficiently to ssRNA by UV, but not MB crosslinking (data not shown). These data therefore suggest that MB crosslinking is specific for dsRNA–protein interactions.

MB is more efficient than UV for crosslinking dsRNA binding proteins

The data presented above show that MB crosslinking can detect interactions of dsRNA with proteins but not interactions of ssRNA with proteins or RNA–RNA base pairing interactions. Our next aim was to compare directly MB crosslinking with conventional UV-induced crosslinking for the detection of dsRNA–protein binding. We used GST-dsRBD and full-length PKR and a

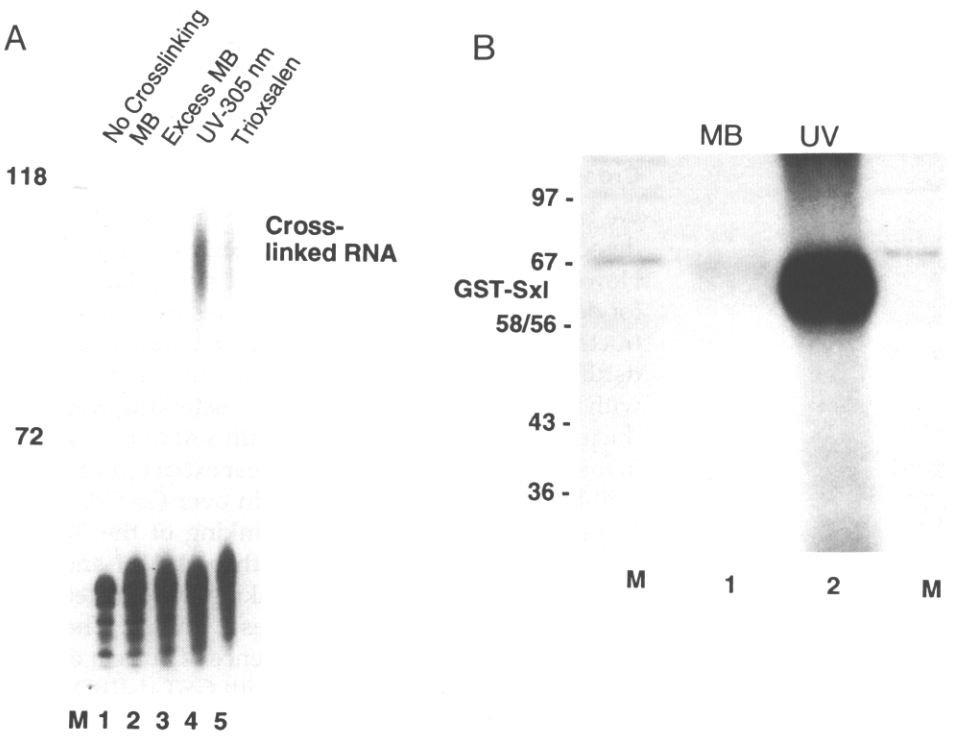

FIGURE 3. MB does not mediate RNA–RNA or ssRNA–protein crosslinking. **A:** Labeled pSP 70/*Bgl* II RNA was hybridized to fivefold excess of unlabeled pSP 70/*Xho* I RNA and the hybrid was treated by the various crosslinking conditions indicated. Lane 1, no crosslinking; lane 2, 5 ng MB; lane 3, 250 ng MB; lane 4, 4-thio U RNA, 305-nm crosslinking; lane 5, trioxsalen crosslinking. Lane M contains labeled ϕX *Hae* III DNA size markers. Positions of the 118- and 72-nt markers are indicated to the left. Crosslinking results were analyzed by 8 M urea 6% PAGE. **B:** Crosslinking of 65-kDa GST-Sxl protein to a 54-nt RNA containing an Sxl binding site by UV light (lane 2) or MB (lane 1). Lane M, molecular weight markers. Sizes of markers are indicated to the left.

series of highly structured RNAs, including VAI, the 3′-UTR of *bicoid* mRNA (a natural substrate for staufen binding), and a 40-bp hybrid of complementary RNAs transcribed from the polylinker region of the pSP70 vector. All of the RNAs bound to GST-dsRBD, as revealed by electrophoretic mobility shifting (data not shown). MB mediated crosslinking of GST-dsRBD to all three RNAs (Fig. 4A, lanes 1, 3, 5). UV light only induced crosslinking with VAI RNA, and this was less efficient than the equivalent MB crosslinking (compare lanes 1 and 2). In contrast, with *bicoid* 3′UTR and the hybrid RNAs, UV crosslinking was barely detectable (lanes 4, 6), whereas MB crosslinking was nearly as efficient as with VAI (lanes 3, 5).

Similar results were obtained with purified human PKR. Binding of PKR to all three RNAs was detected by MB crosslinking and, in each case, the corresponding signal with UV crosslinking was weaker (Fig. 4B). Once again, the relative efficiency of detection with MB compared to UV appeared to be greater for the 40-bp hybrid and *bicoid* than for VAI. This hierarchy reflects the increasing base paired content of the different RNAs. Although VAI contains a substantial proportion of unpaired bases in loops, the polylinker hybrids contain an uninterrupted helix, with short single-stranded regions at the ends of the helix. It has been observed previously that dsRBD proteins contact VAI both at the central domain containing unpaired bases, as well as at the apical stem (Clarke & Mathews, 1995). It is likely that UV light induces crosslinking to GST-dsRBD via these single-stranded regions. These data therefore suggest that, in contrast to UV crosslinking, which occurs preferentially at non-base paired regions, MB crosslinking is dependent upon base paired structure.

The preceding data showed that, for highly structured RNAs, MB crosslinking is more efficient than UV crosslinking. Nevertheless, the levels of MB crosslinking also appeared to be reduced with the perfect duplex compared with VAI (compare lanes 1 and 5, Fig. 4A,B). One reason for the decreased signal with the 40-bp hybrid is that, unlike the VAI and *bicoid* RNAs, only one of the two strands is labeled and, in addition, there was an excess of the unlabeled strand that may have partially competed for MB binding. However, it is possible that MB crosslinking may actually be less efficient with fully base paired dsRNA. To investigate whether fully base paired RNA shows different crosslinking efficiency from a distorted helix, we conducted MB crosslinking experiments with GST-dsRBD and two hybrid RNAs prepared from the polylinker of pBluescript II SK (Fig. 4C). In each case, the [^{32}P-UTP] labeled strand was an *Eco*0109 I run-off transcript from the T3 promoter. The complementary T7-synthesized strands were either derived from the same polylinker, giving an uninterrupted 95-bp duplex, or contained an 8-bp deletion to yield a duplex RNA with an 8-bp bulge in the labeled strand flanked by helices of 24 and 63 bp. Treatment with either 5 ng (lanes 1 and 3) or 25 ng of MB (lanes 2 and 4) produced similar efficiencies of radiolabel transfer for the two duplexes (1.2%, 0.6%, 1%, and 0.8% in lanes 1–4, respectively). Note that these figures are for efficiency of radio-label transfer and

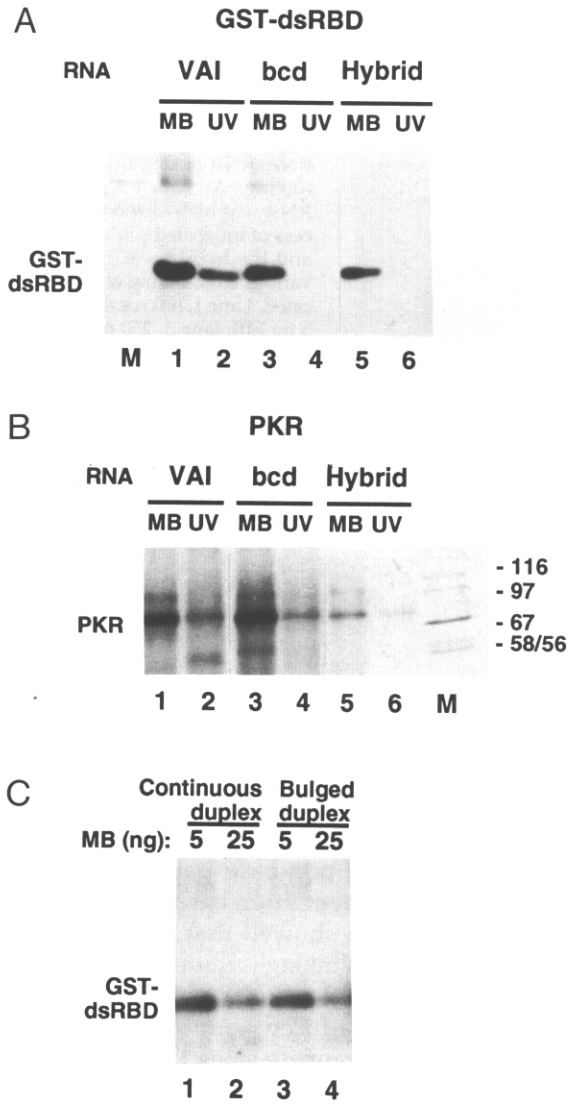

FIGURE 4. Crosslinking of GST-dsRBD and PKR with different RNAs. **A:** GST-dsRBD was incubated with VAI (lanes 1, 2), 3′-UTR of *bicoid* (indicated as bcd, lanes 3, 4), or hybrid pSP70 RNAs (lanes 5, 6). Equal amounts of radiolabeled RNAs of similar specific activity were used. Crosslinking was by MB (lanes 1, 3, 5) or UV (lanes 2, 4, 6). Molecular weight markers are shown (lane M). Position of the crosslinked 37-kDa GST-dsRBD is indicated to the left. **B:** Crosslinking of PKR. Lanes labeled as in A. Position of the crosslinked 68-kDa PKR is indicated to the left. Sizes of markers are indicated on the right. **C:** Comparison of MB crosslinking of GST-dsRBD to an uninterrupted 95-bp duplex (lanes 1, 2) or a duplex with an 8-nt bulge flanked by 24- and 63-bp helices (lanes 3, 4). Crosslinking was conducted in the presence of 5 ng (lanes 1, 3) or 25 ng of MB (lanes 2, 4). Efficiencies of radiolabel transfer from RNA to protein were estimated by phosphorimaging to be 1.2, 0.6, 1.0, and 0.8%, respectively, in lanes 1–4.

should not be compared directly with the 12% crosslinking efficiency estimated for the HP RNA (Fig. 2B); estimation of efficiency of RNA–protein crosslinking would require determination of the number of binding sites for GST-dsRBD within the two RNAs. In each case, the efficiency of crosslinking was reduced at the higher MB concentration, as observed previously for VAI and the 25-bp hairpin (Fig. 2). These data show that the presence of unpaired bases distorting the dsRNA helix does not necessarily increase the efficiency of MB crosslinking.

Crosslinking of target protein in cell extracts

We have shown that MB crosslinking can be used to detect interactions of purified proteins with dsRNA. However, crosslinking methods are particularly useful for detecting RNA–protein interactions in crude cell extracts. We therefore tested whether binding of GST-dsRBD to RNAs could be detected when it was mixed with HeLa cell nuclear extract. Crosslinking was conducted after a short incubation with VAI or *bcd* 3′-UTR, in the presence or absence of nuclear extract (containing a 50-fold weight excess of protein over GST-dsRBD). Figure 5 shows that MB crosslinking of the 37-kDa dsRBD was detected readily with both VAI and *bcd*-UTR (lanes 3 and 8). This crosslinking was not detected with nuclear extract alone (lanes 2 and 7). The efficiency of crosslinking in the presence of nuclear extract was slightly reduced compared with GST-dsRBD alone (compare lanes 1 and 3, 6 and 8). Increasing the concentration of MB failed to restore full crosslinking, suggesting that the reduction in crosslinking intensity is not due to MB binding by unlabeled RNAs in the extract. Neither did prior treatment of the extract with micrococcal nuclease increase the signal, indicating that endogenous dsRNAs in the extract are not binding significant amounts of the GST-dsRBD. The most likely explanation for the reduced signal is competition for the labeled RNA probe by other proteins in the nuclear extract. These proteins, many of which would contain more than one dsRBD, would likely bind with higher affinity than the GST-dsRBD. Three nuclear proteins were detected by MB crosslinking with apparent molecular sizes of 47 kDa, 97 kDa, and ~132 kDa (lanes 2 and 7). UV-induced crosslinking detected many other proteins in the nuclear extract, which made it difficult to distinguish whether the GST-dsRBD had been crosslinked (lanes 4, 5, 9, 10). It is apparent that many more proteins are detected by UV than by MB crosslinking of the extract alone (lanes 2, 4, 7, 9). It is likely that the few extract proteins detected by MB crosslinking bind specifically to dsRNA. Consistent with this, we found that, although many of the UV-crosslinked bands could be competed by unlabeled homoribopolymers, most of the MB-crosslinked bands were resistant to competition (data not shown). These data therefore suggest that MB crosslinking may be useful as a discriminating technique for the detection of dsRNA-binding proteins in crude extracts.

DISCUSSION

We have described here a novel method for RNA–protein crosslinking that specifically detects proteins

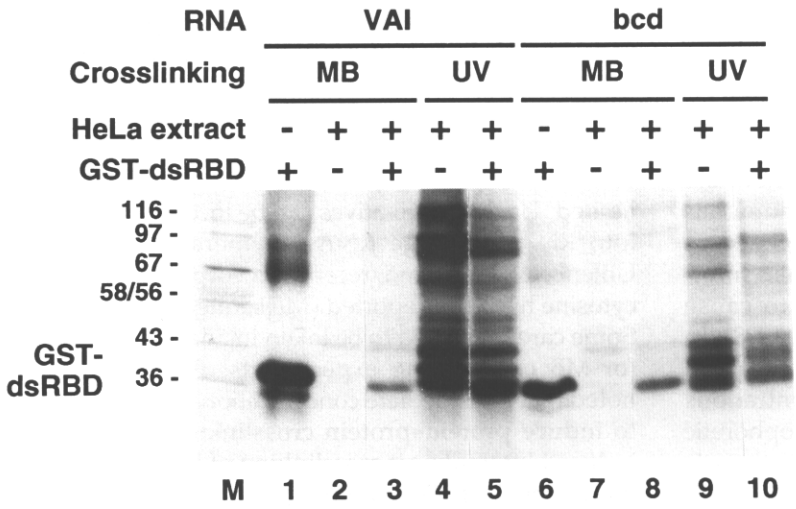

FIGURE 5. Crosslinking in HeLa nuclear extracts. GST-dsRBD was crosslinked to VAI (lanes 1–5) and to 3′-UTR of *bicoid* (lanes 6–10) in the presence or absence of 12% HeLa nuclear extract (indicated above lanes). GST-dsRBD (150 ng) was mixed with 1.2 μL of HeLa nuclear extract (7.3 μg protein), then 6 ng of labeled VAI or 3′-UTR of *bicoid* RNA were added to a total volume of 10 μL. After a short incubation, the mixtures were subjected to either MB (lanes 1–3, lanes 6–8) or UV light (lanes 4, 5 and 9, 10) crosslinking (see the Materials and methods). Sizes of molecular weight markers (lane M) are shown to the left.

interacting with dsRNA. This is in contrast to the widely used UV-crosslinking methods in which crosslinking to double-stranded regions is often relatively inefficient. The low efficiency is likely because the photoactivated base intermediates react preferentially with their base paired partners rather than with amino acid residues of bound proteins. UV crosslinking of dsRNA-binding proteins may therefore actually rely upon the presence of some unpaired bases (Fig. 4). In contrast, MB treatment produced crosslinking efficiencies of 10–15% (Fig. 2B) with highly structured RNAs. Because all of the RNAs used in the experiments reported here contained some nonpaired bases, either as terminal single-stranded overhangs or internal loops and bulges, we cannot rule out the possibility that MB crosslinking may require the presence of some unpaired bases. Nevertheless, this seems an unlikely possibility. First, the 40-bp hybrid RNA in Figure 4A and B contained only four unpaired bases on the labeled strand and none of these carried ^{32}P label. The apparently lower crosslinking efficiency of the hybrid RNA compared to the VAI and *bicoid* RNAs can be attributed at least in part to the fact that only one of the two strands of the hybrid was labeled and that the unlabeled strand was present in excess, potentially binding some MB. In contrast, UV crosslinking of the GST-dsRBD to the hybrid RNAs was undetectable (Fig. 4A). Second, we observed no difference in efficiency of MB crosslinking in hybrid RNAs that formed an uninterrupted helix, compared with a similar duplex with an 8-bp bulge (Fig. 4C). Third, we detected efficient crosslinking of GST-dsRBD to a continuous 25-bp stem (Fig. 2C); again, the 4-bp loop in this experiment contained no labeled nucleotides. Finally, when we have compared MB- and UV-induced crosslinking reactions with ssRNA and either purified sex-lethal (Fig. 3) or La protein, or in HeLa nuclear extracts (data not shown), the efficiency of UV-induced RNA–protein crosslinking has always been far greater than with MB. These data all suggest that the MB-crosslinking method is specific for dsRNA–protein interactions, although the possibility remains that unpaired bases may in some cases be able to enhance the efficiency of crosslinking.

Most biophysical studies on the interaction of MB with nucleic acids have been carried out with DNA. MB binds to double-stranded nucleic acids predominantly by intercalation, with a preference for G-C base pairs. Intercalation to poly (dGdC) (binding constant, $K_a = 1.6 \times 10^6\ M^{-1}$) has a 100-fold higher affinity than with poly (dAdT), and, in the latter case, surface binding contributes equally (Atherton & Harriman, 1993). The dye also binds to single-stranded nucleic acids, with an affinity an order of magnitude lower, predominantly via electrostatic interaction of the cationic dye with the phosphate backbone. (Hagmar et al., 1992; Antony et al., 1993). MB has been used previously to induce DNA–histone crosslinking in chromatin, and this was shown to be dependent upon MB intercalation by competition of crosslinking with ethidium bromide (Lalwani et al., 1990, 1995). The dye appeared to act as a mediator rather than forming the crosslinks directly. The chemical mechanism by which MB mediates crosslinking remains unclear, although photosensitization of DNA occurs specifically at guanine bases (reviewed in Tuite & Kelly, 1993). The mechanism is clearly distinct from that of UV-induced crosslinking because MB can mediate RNA–protein, but not RNA–RNA crosslinking of dsRNA. This suggests that the photo-activated groups do not reside on the inaccessible major groove side of the base pairs. The fact that we have been able to use MB for crosslinking proteins to dsRNA suggests that the precise geometry of the double helix (A-form RNA compared to B-form DNA) is not important for MB binding and crosslinking. Although we did not formally demonstrate that MB crosslinking to dsRNA was dependent upon MB intercalation, this seems the most

reasonable explanation given the dependence of the method upon the double-stranded character of the RNA (Figs. 3, 4).

At present, there remain a number of unanswered questions about the MB-crosslinking technique and the factors that may affect its efficiency. First, it is not clear precisely what structural effects MB intercalation has upon the geometry of the dsRNA helix, and what consequences these may have upon RNA–protein interactions. Intercalative binding is expected to cause partial unwinding of the helix (Tuite & Kelly, 1993). In the case of the staufen GST-dsRBD, we have observed that MB does not affect binding at the concentrations used for crosslinking, as determined by electrophoretic mobility shift assay. Only at higher concentrations is protein binding inhibited, as determined by both MB crosslinking (Fig. 2) and gel-shift assays. A reasonable interpretation of these data is that high MB concentrations interfere with protein binding due to either competition for electrostatic binding of the positively charged MB to the phosphate backbone or distortion of helix geometry by high occupancy of intercalation sites. At the approximately optimal ratio of MB to VAI RNA of 2:6 ng (Fig. 2), the molar ratio of MB (molecular weight 320) to RNA bases is 1:3, and to RNA base pairs is 1:1. However, the total concentrations of MB and base pairs (~0.6 μM) are close to the dissociation constant for the binding of MB to poly (dGdC) (Atherton & Harriman, 1993), so the actual amount of MB intercalated is most likely substantially less than 1 per base pair. It may be that the empirically determined optimal concentration of MB reflects a relatively low occupancy of intercalation sites with little attendant distortion of the helix geometry. It remains to be determined whether other dsRNA-binding proteins will be sensitive to the levels of MB required for effective crosslinking.

Another open question is whether crosslinking, in addition to binding of MB, shows any marked sequence preferences. Photosensitization of DNA by methylene blue involves modifications specifically at guanine bases (Tuite & Kelly, 1993), and this is likely to hold for RNA. The HP RNA (Fig. 2B) contains a stem with 24 G-C base pairs and a single A-U pair, and crosslinks with an efficiency of ~12%. We have also tested crosslinking of GST-dsRBD to a 30-bp stem composed purely of AU base pairs, except for two GC pairs introduced by the polylinker *Pvu* II site; although quantitative measurements of efficiency have not been made, crosslinking was observable readily with the AU-rich stem (Z.-R. Liu & C.W.J. Smith, unpubl. obs.). Thus, it is likely that MB crosslinking may have fairly flexible sequence requirements. Given that most dsRNA-binding proteins show little sequence specificity for binding, it is unlikely that many dsRNA probes would be ineffective for MB crosslinking. In this respect, MB detection of dsRNA-binding proteins promises to be at least as flexible as other crosslinking approaches. For instance, UV-induced crosslinking occurs mainly to uracil bases with a small amount to cytidine (Smith, 1976; Hockensmith et al., 1986). Also, the availability of photoreactive nucleotide analogues that are known to be efficiently incorporated by RNA polymerases is limited. Uridine derivatives can be incorporated readily into RNA by phage RNA polymerases (Milligan & Uhlenbeck, 1989), and, recently, incorporation of 5-iodocytosine has been reported (Meisenheimer et al., 1996). Some care may need to be taken in adapting conditions for MB crosslinking experiments. For instance, we noted that intermediate concentrations of MB appeared to induce protein–protein crosslinking (Fig. 2). MB-induced intersubunit crosslinking of both hemoglobin (Girotti et al., 1979) and myoglobin (Van Steveninck & Dubbelman, 1984) has been observed previously, so preliminary titrations may be advisable to determine the optimal MB concentration for a particular RNA–protein crosslinking experiment. Finally, it may be advisable to avoid buffers containing EDTA, which photoreduces the excited triplet state of MB. This could potentially both decrease dye-mediated crosslinking, as well as produce damaging radicals (Tuite & Kelly, 1993). These minor caveats notwithstanding, it is worth noting that we obtained all of the data presented here using illumination by a standard domestic fluorescent tube light, so it is likely that refinements to the procedure will allow for improved efficiencies of crosslinking.

The method reported here has potentially advantageous applications in the study of a number of important biological processes. Our motivation was to develop a site-specific crosslinking procedure that would detect proteins interacting with only the double-stranded region of a largely ssRNA transcript. The second step of pre-mRNA splicing exhibits some characteristics that are consistent with a 5′ to 3′ scanning process from the branch point to the first AG dinucleotide. Stable secondary structure inserted between the branch point and 3′ splice site specifically blocks step 2 of splicing (Smith et al., 1989, 1993). We have used the MB-crosslinking procedure in an attempt to detect spliceosome components that have been blocked by the secondary structure, and have identified a 118-kDa protein that appears to be a candidate step 2 splicing factor (Z.-R. Liu & C.W.J. Smith, unpubl. obs.). Many other applications of the MB crosslinking procedure can be conceived. Double-stranded RNA-binding proteins are involved in various cellular functions including signal transduction, control of transcription and translation, and anti-viral responses. Among the enzymes known to act upon, or to be activated by, dsRNA are PKR (Proud, 1995; Clemens, 1996), dsRNA adenosine deaminase (Hough & Bass, 1994; Patterson et al., 1995), and the various isoforms of 2′-5′ oligoadenylate synthetase (Witt et al., 1993), all of which are induced by interferons. The MB crosslinking method

may be useful in the investigation of these proteins, as well as in the identification of hitherto unknown dsRNA interacting proteins.

MATERIALS AND METHODS

Chemicals and enzymes

Methylene blue was purchased from BDH and was used without further purification. The compound was dissolved in water as a 2.5 mg/mL stock solution. The concentration was determined by $\epsilon_{665nm} = 81{,}600\ cm^{-1}\ M^{-1}$. Trioxsalen was purchased from Sigma and was used without further purification. The compound was dissolved in ethanol as a saturated solution. 4-thio-UTP was a gift from Carola Lempke and Richard Jackson. All the restriction enzymes and other enzymes were purchased from New England Biolabs, Pharmacia, or Boehringer, and were used following the manufacturers' instructions.

RNAs

All RNAs were transcribed from the appropriate linearized plasmid with T7, SP6, or T3 RNA polymerase using an m7G(5′)ppp(5′)G dinucleotide primer. The RNAs were radiolabeled with the appropriate [α^{32}P]-NTP. The vectors for transcribing the 3′-UTR of *bicoid* RNA and VAI RNA were kindly provided by Dr. Stefan Grünert (Bycroft et al., 1995). The RNA HP (Fig. 2B) was transcribed from a pSP70 vector in which the following sequence had been cloned into the *Pvu* II site: 5′-GGG(CGG)$_6$ GAATTC(CCG)$_6$ CCC-3′. The resultant [α ^{32}P-CTP]-labeled SP6 *Hin*d III run-off transcripts contained a predicted 25-bp stem consisting of 24 G-C base pairs and a single A-U base pair, a 4-nt AAUU loop, and 9-nt 5′ and 5-nt 3′ single-stranded tails. For GST-Sxl binding, a 54-nt RNA containing the sequence, 5′-UUUUUGUUGUUU UUUUUCU-3′, which is an Sxl-binding site in *tra* pre-mRNA (Valcárcel et al., 1993), was transcribed from a Bluescript SKII plasmid. pSP70 is a commercial plasmid from Promega. For transcription of RNA containing 4-thio U (Fig. 3), UTP was replaced by 4-thio-UTP. The RNAs used to compare the efficiency of MB crosslinking with perfect and distorted helices (Fig. 4C) were transcribed from pBluescript II SK. The T3 transcribed strand was labeled using [α-^{32}P]-UTP and was run-off at the *Eco*0109 I site. The complementary T7 strands were terminated at a blunted *Sac* I site. For the bulged duplex, the template vector had an 8-bp deletion between the *Xba* I and *Bam*H I sites. The resultant hybrids had a 16-nt 5′ overhang of the labeled strand and a 14-nt 5′ overhang of the unlabeled strand. The uninterrupted duplex consisted of 95 bp, whereas the other duplex had an 8-bp bulge flanked by 24- and 63-bp helices.

Proteins

Expression vectors for GST-dsRBD of staufen and its mutant F32A were kindly provided by Dr. Stefan Grünert (Bycroft et al., 1995). The vectors were transformed into *E. coli*. An overnight mini-culture was diluted 10 times and grown for another 2 h. IPTG was then added to 0.1 mM to induce expression. After an additional 3 h, the cells were harvested and resuspended in 1/100 volume of phosphate-buffered saline. Bacterial cells were lysed by sonicating on ice for 2 × 40 s using a microtip. The lysed cells were pelleted in a microcentrifuge for 4 min. Triton X-100 (1%) was added to the supernatant, which was then mixed with 100 μL of Glutathione-Sepharose slurry (Pharmacia) on ice for 1 h. After washing, the protein was eluted with 5× bed volume of 50-mM glutathione in 100 mM Hepes, pH 8.0. GST-Sxl protein was provided by Clare Gooding and was expressed using vectors that were kindly provided by Juan Valcárcel and Michael Green (Valcárcel et al., 1993). The HeLa cell nuclear extracts were prepared as described previously (Mullen et al., 1991).

PKR was prepared from *Spodoptera frugiperda* cells infected with a recombinant baculovirus containing a full-length PKR cDNA (kindly provided by Drs. Glen Barber and Dirk Gewert) as described previously (Sharp et al., 1993). The PKR contained a point mutation (Lys 296 to Arg 296) that abolishes the catalytic activity but does not abolish the dsRNA-binding properties of the protein kinase (Katze et al., 1991; Barber et al., 1992).

Electrophoretic mobility shift assay

Appropriate amounts of RNA (5 ng VAI) were incubated with 100–150 ng of protein at room temperature in 10-μL diluted protein storage buffer (final concentrations: 3 mM Tris, pH 7.5, 0.75% glycerol, 15 mM KCl, 0.03 mM EDTA, and 0.075 mM DTT). Four microliters of loading buffer (30% glycerol, 0.25% bromophenol blue, 0.25% xylene cyanol) were added to the samples, which were then loaded onto an 8% native polyacrylamide gel (0.5× TBE, acrylamide:bisacrylamide = 60:1). Electrophoresis was performed at a constant voltage of 200 V in 0.5× TBE buffer.

Methylene blue crosslinking

Appropriate amounts of RNAs (~5 ng) were mixed with 100–150 ng of proteins (or appropriate percentage of HeLa nuclear extract and protein mixture) in a total volume of 10 μL (same buffer as for gel mobility shift assay above). Methylene blue was added into the solution to 0.2–1 ng/μL. After a short incubation at room temperature, the mixture was placed in a micro-titre plate. The plate was then placed 4–5 cm below a 60 W fluorescent tube light. The crosslinking was conducted on ice for ~20 min. The mixture was then digested with RNase A (1 $\mu g \cdot \mu L^{-1}$), RNase T1 (0.3 $U \cdot \mu L^{-1}$), and RNase V1 (0.035 $U \cdot \mu L^{-1}$), at 37 °C for 20 min. Crosslinking results were analyzed by electrophoresis on 20% polyacrylamide SDS gels. Molecular size standards for SDS gels had the following molecular weights (kDa): 116.4, 97.1, 66.5, 57.6, 55.6, 43.1, 35.7, 29.0, 13.7.

To calculate the efficiency of MB crosslinking (Fig. 2B), binding reactions were conducted using the RNA HP, which would be expected to bind a single dsRBD. Reactions were performed under conditions of protein excess in which all the RNA was in the bound state. Samples of the undigested RNA were run alongside the crosslinked samples and quantitated using a Molecular Dynamics PhosphorImager, allowing di-

rect measurement of the percentage of radiolabel transfer from RNA to protein. Crosslinking efficiencies were calculated by multiplying the percentage of label transfer by the number of labeled CMP residues in the RNA, on the assumption that a single radio-labeled phosphate was transferred during crosslinking. If more than one label was transferred, then the estimate of crosslinking efficiency would be reduced accordingly.

UV-induced crosslinking

Appropriate amounts of RNAs (~5 ng) were mixed with 100–150 ng of proteins (or appropriate percentage of HeLa nuclear extract and protein mixture) in 10-μL total volume. After a short incubation at room temperature, the mixture was placed in a micro-titre plate. The samples were irradiated under 254-nm light in a crosslinker (Spectronic) using 1.72 J cm^{-1} light dosage. Analysis of crosslinking followed the same procedure as above for MB crosslinking.

RNA–RNA hybridization and crosslinking

RNA hybrids were formed with 52-nt and 44-nt transcripts derived from the polylinker of pSP70 after digestion of the plasmid with *Xho* I or *Bgl* II, respectively. The resultant hybrid RNA had 40 bp of uninterrupted double-stranded helix with single-stranded 5′ overhangs of 4 and 12 nt at the ends. Annealing of complementary RNAs was performed by incubating at 65 °C for 4 min followed by slow cooling. Three nanograms of [^{32}P]-labeled pSP 70/*Bgl* II transcript were hybridized to fivefold excess of unlabeled pSP 70/*Xho* I transcript. The annealed hybrid was incubated in 10 mM Tris, pH 7.8, 2.5 mM $MgCl_2$ prior to crosslinking. For RNA–RNA crosslinking with 4-thio-U containing RNA, irradiation was on a UV-transilluminator (305 nm, 4 × 15 W) for 8 min. For trioxsalen crosslinking, 1 μL of trioxsalen-saturated ethanol was added to 10 μL RNA hybrid. The mixture was irradiated on a transilluminator (365 nm, 4 × 15 W) for 8 min. MB crosslinking was conducted as for RNA–protein crosslinking with either 5 ng or 250 ng of MB in a 10-μL reaction volume. Crosslinking results were analyzed by 6% urea-PAGE.

ACKNOWLEDGMENTS

We thank Drs. Stefan Grünert and Daniel St. Johnston for supplying the vectors for expression of the staufen GST-dsRBDs and the VAI and *bcd* RNAs, Juan Valcárcel and Michael Green for supplying vectors for expression of GST-Sxl, Clare Gooding for preparing the recombinant GST-Sxl, and Drs. Glen Barber and Dirk Gewert for the recombinant baculovirus expressing PKR and for help in the purification of the protein. We thank Carola Lempke and Richard Jackson for the gift of 4-thio UTP, and Gavin Roberts for comments on the manuscript. This work was supported by grants from the Wellcome Trust to C.W.J.S. and from the Cancer Research Campaign and Wellcome Trust to M.J.C. A.W. holds a Research Studentship from the Medical Research Council.

Received January 26, 1996; returned for revision March 1, 1996; revised manuscript received May 1, 1996

REFERENCES

Antony T, Atreyi M, Rao MVR. 1993. Spectroscopic studies on the binding of methylene blue to poly(riboadenylic acid). *J Biomol Struct Dynam 11*(1):67–81.

Atherton SJ, Harriman A. 1993. Photochemistry of intercalated methylene blue. Photoinduced hydrogen-atom abstraction from guanine and adenine. *J Am Chem Soc 115*:1816–1822.

Barber GN, Tomita J, Garfinkel MS, Meurs E, Hovanessian A, Katze MG. 1992. Detection of protein kinase homologues and viral RNA-binding domains utilizing polyclonal antiserum prepared against a baculovirus-expressed dsRNA-activated 68,000-Da protein kinase. *Virology 191*:670–679.

Bass BL. 1995. RNA editing—An I for editing. *Curr Biol 5*(6):598–600.

Bass BL, Hurst SR, Singer JD. 1994. Binding properties of newly identified *Xenopus* proteins containing dsRNA-binding motifs. *Curr Biol 4*(4):301–314.

Bycroft M, Grünert S, Murzin AG, Proctor M, St. Johnston D. 1995. NMR solution structure of a dsRNA binding domain from *Drosophila* Staufen protein reveals homology to the N-terminal domain of ribosomal protein S5. *EMBO J 14*(14):3563–3571.

Cattaneo R. 1994. RNA duplex guide base conversions. *Curr Biol 4*(2): 134–136.

Chan EKL, Tan EM. 1987. The small nuclear ribonucleoprotein SS-B/La binds RNA with a conserved protease-resistant domain of 28 kilodaltons. *Mol Cell Biol 7*:2588–2591.

Clarke PA, Mathews MB. 1995. Interactions between the double-stranded RNA binding motif and RNA: Definition of the binding site for the interferon-induced protein kinase DAI (PKR) on adenovirus VA RNA. *RNA 1*(1):7–20.

Clemens MJ. 1996. Protein kinases that phosphorylate eIF2 and eIF2B, and their role in eukaryotic cell translational control. In: Hershey JWB, Mathews MB, Sonenberg N, eds. *Translational control*. Cold Spring Harbor, New York: Cold Spring Harbor Laboratory Press. pp 139–172.

Clemens MJ, Laing KG, Jeffrey IW, Schofield A, Sharp TV, Elia A, Matys V, James MC, Tilleray VJ. 1994. Regulation of the interferon-inducible eIF-2α protein kinase by small RNAs. *Biochimie 76*:770–778.

Ferrandon D, Elphick L, Nüsslein-Volhard C, St. Johnston D. 1994. Staufen protein associates with the 3′ UTR of *bicoid* mRNA to form particle that moves in a microtubule-dependent manner. *Cell 79*:1221–1232.

Girotti AW, Lyman S, Deziel MR. 1979. Methylene blue-sensitized photo-oxidation of hemoglobin: Evidence for cross-link formation. *Photochem Photobiol 29*:1119–1125.

Gott JM, Willis MC, Koch TH, Uhlenbeck OC. 1991. A specific UV-induced RNA–protein cross-link using 5-bromouridine-substituted RNA. *Biochemistry 30*(25):6290–6295.

Gottlieb E, Steitz JA. 1989. Function of the mammalian La protein—Evidence for its action in transcription termination by RNA polymerase III. *EMBO J 8*:851–861.

Green SR, Manche L, Mathews MB. 1995. Two functionally distinct RNA-binding motifs in the regulatory domain of the protein kinase DAI. *Mol Cell Biol 15*(1):358–364.

Hagmar P, Pierrou S, Nielsen P, Norden B, Kubista M. 1992. Ionic strength dependence of the binding of methylene blue to chromatin and calf thymus DNA. *J Biomol Struct Dynam 9*(4):667–679.

Hanna MM. 1989. Photoaffinity cross-linking methods for studying RNA–protein interaction. *Methods Enzymol 180*:383–490.

Hockensmith JW, Kubasek WL, Vorachek WR, von Hippel PH. 1986. Laser cross-linking of nucleic acids to proteins. *J Biol Chem 261*(8): 3521–3518.

Hough RF, Bass BL. 1994. Purification of the *Xenopus laevis* double-stranded RNA adenosine deaminase. *J Biol Chem 269*:9933–9939.

Jagus R, Gray MM. 1994. Proteins that interact with PKR. *Biochimie 76*:779–791.

Katze MG, Wambach M, Wong ML, Garfinkel M, Meurs E, Chong K, Williams BRG, Hovanessian AG, Barber GN. 1991. Functional expression and RNA binding analysis of the interferon-induced double-stranded RNA-activated, 68,000-Mr protein kinase in a cell-free system. *Mol Cell Biol 11*:5497–5505.

Kharrat A, Macias MJ, Gibson TJ, Niges M, Pastore A. 1995. Structure of the dsRNA binding domain of *E. coli* RNase III. *EMBO J 14*: 3572–3584.

Lalwani R, Maiti S, Mukherji S. 1990. Visible light induced DNA–

protein crosslinking in DNA–histone complex and sarcoma-180 chromatin in the presence of methylene blue. *J Photochem Photobiol B 7*:57–73.

Lalwani R, Maiti S, Mukherji S. 1995. Involvement of H1 and other chromatin proteins in the formation of DNA–protein crosslinks induced by visible light in the presence of methylene blue. *J Photochem Photobiol B 27*:117–122.

MacMillan AM, Query CC, Allerson CR, Chen S, Verdine GL, Sharp PA. 1994. Dynamic association of proteins with the pre-mRNA branch region. *Genes & Dev 8*:3008–3020.

Meisenheimer KM, Meisenheimer PL, Willis MC, Koch TH. 1996. High yield photocrosslinking of a 5-iodocytidine (IC) substituted RNA to its associated protein. *Nucleic Acids Res 24*:981–982.

Milligan JF, Uhlenbeck OC. 1989. Synthesis of small RNAs using T7 RNA polymerase. *Methods Enzymol 180*:51–62.

Moore MJ, Sharp PA. 1992. Site-specific modification of pre-mRNA: The 2′-hydroxyl groups at the splice site. *Science 256*:992–997.

Mullen MP, Smith CWJ, Patton JG, Nadal-Ginard B. 1991. α-Tropomyosin mutually exclusive exon selection: Competition between branchpoint/polypyrimidine tracts determines default exon choice. *Genes & Dev 5*:642–655.

Patterson JB, Thomis DC, Hans SL, Samuel CE. 1995. Mechanism of interferon action. Double-stranded RNA-specific adenosine-deaminase from human cells is inducible by α-interferon and γ-interferon. *Virology 210*:508–511.

Proud CG. 1995. PKR: A new name and new roles. *Trends Biochem Sci 20*:241–246.

Sharp TV, Xiao Q, Jeffrey I, Gewert DR, Clemens MJ. 1993. Reversal of the dsRNA-induced inhibition of protein synthesis by an inactive mutant of the protein kinase PKR. *Eur J Biochem 214*: 945–948.

Singh R, Valcárcel J, Green MR. 1995. Distinct binding specificities and functions of higher eukaryotic polypyrimidine tract-binding protein. *Science 268*:1173–1176.

Smith CWJ, Chu TT, Nadal-Ginard B. 1993. Scanning and competition between AGs are involved in 3′ splice site selection in mammalian introns. *Mol Cell Biol 13*:4939–4952.

Smith CWJ, Porro EB, Patton JG, Nadal-Ginard B. 1989. Scanning from an independently specified branch point defines the 3′ splice site of mammalian introns. *Nature 342*:243–247

Smith KC. 1976. *Photochemistry and photobiology of nucleic acids*. New York: Academic Press. pp 187–218.

Stebbings H, Lane JD, Talbot NJ. 1995. mRNA translation and microtubules: Insect ovary models. *Trends Cell Biol 5*:361–365.

St. Johnston D. 1995. The intracellular localization of messenger RNAs. *Cell 81*:161–170.

St. Johnston D, Beuchle D, Nüsslein-Volhard C. 1991. *Staufen*, a gene required to localize maternal RNAs in the *Drosophila* egg. *Cell 66*:51–63.

St. Johnston D, Brown NH, Gall JG, Jantsch M. 1992. A conserved double-stranded RNA-binding domain. *Proc Natl Acad Sci USA 89*:10979–10983.

Tanner NK, Hanna MM, Abelson J. 1988. Binding interaction between yeast tRNA ligase and a precursor transfer ribonucleic acid containing two photoreactive uridine analogues. *Biochemistry 27*(24):8852–8861.

Tuite E, Norden B. 1994. Sequence-specific interactions of methylene-blue with polynucleotides and DNA—A spectroscopic study. *J Am Chem Soc 116*:7548–7556.

Tuite EM, Kelly JM. 1993. Photochemical interactions of methylene blue and analogues with DNA and other biological substrates. *J Photochem Photobiol B 21*:103–124.

Valcárcel J, Singh R, Zamore PD, Green MR. 1993. The protein sex-lethal antagonizes the splicing factor U2AF to regulate alternative splicing of *transformer* pre-mRNA. *Nature 362*:171–175.

Van Steveninck J, Dubbelman TMAR. 1984. Photodynamic intramolecular crosslinking of myoglobin. *Biochim Biophys Acta 791*: 98–101.

Wang J, Bell LR. 1994. The sex-lethal amino terminus mediates cooperative interactions in RNA binding and is essential for splicing regulation. *Genes & Dev 8*:2072–2085.

Weeks KM, Crothers DM. 1993. Major groove accessibility of RNA. *Science 261*:1574–1577.

Willis MC, Hicke BJ, Uhlenbeck OC, Cech TR, Koch TH. 1993. Photocrosslinking of 5-iodouracil-substituted RNA and DNA to proteins. *Science 262*:1255–1257.

Witt PL, Marie I, Robert N, Irizarry A, Borden EC, Hovanessian AG. 1993. Isoforms p69 and p100 of 2′,5′-oligoadenylate synthetase induced differentially by interferons in vivo and in vitro. *J Interferon Res 13*:17–23.

Wower J, Rosen KV, Hixson SS, Zimmermann RA. 1994. Recombinant photoreactive tRNA molecules as probes for cross-linking studies. *Biochimie 76*:1235–1246.